Development of a Vibration-Based Health Monitoring Procedure using a Virtual Axial Piston Pump

Undergraduate Honors Thesis

Presented in Partial Fulfillment of the Requirements for

Graduation with Honors Research Distinction in the

Department of Mechanical and Aerospace Engineering at

The Ohio State University

By:

Valerie A. Yoder

Advisor: Dr. Rajendra Singh

Co-Advisor: Dr. Jason T. Dreyer

****

The Department of Mechanical and Aerospace Engineering

The Ohio State University

April 17, 2015

Thesis Committee:

Dr. Rajendra Singh

Dr. Jason T. Dreyer

Dr. Blaine Lilly

Abstract

Monitoring vibration signatures produced by axial piston pumps can provide insight into changes of the pump system, which may then be associated with early signs of mechanical or hydraulic component failures. To replicate these conditions using physical experiments and sensor-based measurements on pumps is often costly and time-consuming. Therefore, in order to better understand the failure mechanisms, specifically of the swash plate bearing, simulation models are constructed to develop a vibration-based health monitoring procedure to predict hydrostatic bearing failure within an axial piston pump. First, a one-dimensional multi-physics model of an axial piston pump is developed with a representation of the swash plate bearing interface. Next, a series of physical and virtual experiments is designed and used to obtain parameters for this model; these include measured transfer functions that relate housing accelerations to dynamic forces. The model is then utilized to quantify dynamic hydraulic and mechanical loads within the pump as well as to estimate acceleration on the pump housing under a variety of operating conditions. Finally, by detecting changes in acceleration spectra due to a simulated failure, a robust vibration-based health monitoring metric is defined. The resulting metric seems to consistently detect hydrostatic bearing failure under a wide range of pump operating conditions; it is somewhat insensitive to variations in model parameters. This research could ultimately be used by agricultural,

industrial, and aerospace pump manufacturers to gain insights into preventative maintenance guidelines, to identify the least damaging and quietest pump operating regimes, and to screen design concepts before building prototypes.

Acknowledgements

This work has been a tremendous opportunity. I could not have asked for a better to laboratory to work in or a more benevolent mentor to guide me in this research. To this end, I owe both Dr. Rajendra Singh and Dr. Jason Dreyer a great deal of thanks for this opportunity, for their patience, and for their support. I would also like to thank Dr. Blaine Lilly for taking the time to review this thesis and for being a member of my defense committee. Furthermore, I would like to thank NSF I/UCRC Smart Vehicle Concepts Center and Eaton Corporation for their support of this project.

Table of Contents

List of Figures

List of Tables

Chapter 1: Introduction

1.1. Pump Operation and Layout

Variable displacement axial piston pumps (also referred to as swash plate pumps) are used in a variety of aerospace, agricultural, and industrial equipment as either a hydraulic pump or motor. Such applications include aerospace actuators, air conditioning compressors, power washers, industrial hydraulic power sources, and tractor and combine motors [1]. These pumps are often used in these applications since their integrated control circuits allow rest of hydraulic system to be simple and inexpensive.

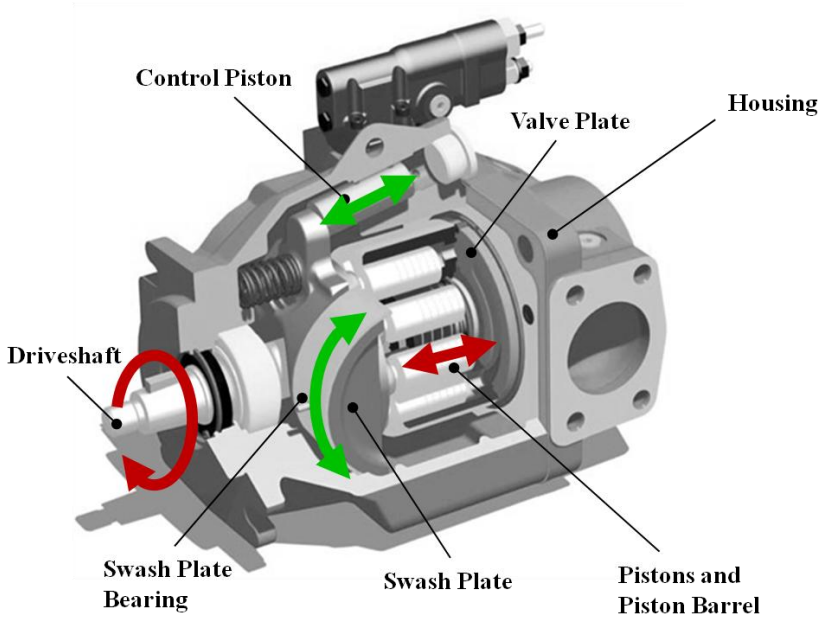

Figure 1. Variable Displacement, Closed Circuit Axial Piston Pump Unit [1]

These pumps pressurize and move fluid by means of a few simple parts: a swash plate, drive shaft, and axial displacement pistons, shown in Figure 1. The pistons in the pumps are axially constrained within a cylinder block that is free to rotate about the same axis in which those pistons move [2]. As the cylinder block is driven by the drive shaft, these pistons move in and out of the cylinder block by following the surface of an angled swash plate. The rotational speed of the shaft and the angle of the plate dictate the volumetric flow rate of the pump. The swash plate can be angled by means of the control piston. The arrangement of the pistons upon the angled swash plate is such that the lower side is below the intake of the pump, which draws in fluid. The pistons then move the fluid to the higher side of the pump, where it is pumped out.

1.2. Vibration-Based Health Monitoring

These pumps typically include an odd number of pistons. For a 9-piston pump, the number of pistons being pressurized at the pump's discharge point will be either 4 or 5 at a given time in a piston barrel cycle, a change which creates pressure ripples or dynamic variations about the generated hydrostatic pressure. This hydraulic load variation will also transmit mechanical loads to the pump housing through the mechanical constraints of the hydraulic components. The torque fluctuation caused by interactions between the rotational drive systems also affects the hydraulic and mechanical loads. It is from these dynamic loads that the structure-borne noise and vibration originate.

Monitoring dynamic signatures produced by the pump can provide insight into changes of the pump system, which can then be associated with early signs of mechanical or hydraulic component failures. Vibration-based health monitoring procedures are

commonly applied to rotating equipment, which incorporate bearing elements. These procedures typically use accelerometers attached to non-rotating structures near the bearings to measure an instantaneous dynamic signature of the system under operating conditions. Comparison of the signature (in time or frequency domain) to a reference or healthy baseline signature provides signs of changes in the dynamic system. Within the axial piston pump shown in Figure 1, there are tapered roller bearings on the shaft and a hydrostatic bearing on the swash plate. Mechanical signatures specific to roller bearing failures are well documented [3], often as additional frequency components that are multiples of the fundamental rotational speed; however, these may overlap with the rich dynamic signature of the pump, making them difficult to distinguish. Other failures within the hydro-mechanical system may include excessive wear of surfaces, misalignments of the rotational components, or cavitation within a pump. All of these will have their own dynamic signatures.

1.2. Swash Plate Bearing Interface

Defining failure of the swash plate bearing interface shown in Figure 1 is more complex than defining failure that originates in a standard rolling element bearing. For the swash plate bearing, the physical mechanisms may not necessarily manifest as additional frequencies in the observed source spectra, as in rolling element bearings. In order to predict failure at the interface of the swash plate bearing, one must fully understand its effect on forces transmitted through different paths within the pump. For this pump configuration, the swash plate has two orifices located on the top side, which guides the pistons. The pistons each have an orifice and reservoir on the bottom to allow

pressurized fluid within the piston to flow to the piston-swash plate interface for lubrication. When the pistons pass over the orifices on the swash plate, pressurized fluid flows to the swash plate bearing interface. This pump has two swash plate bearing interfaces: one at the high pressure (discharge) side and one at the low pressure (intake) side of the pump, illustrated in Figure 2.

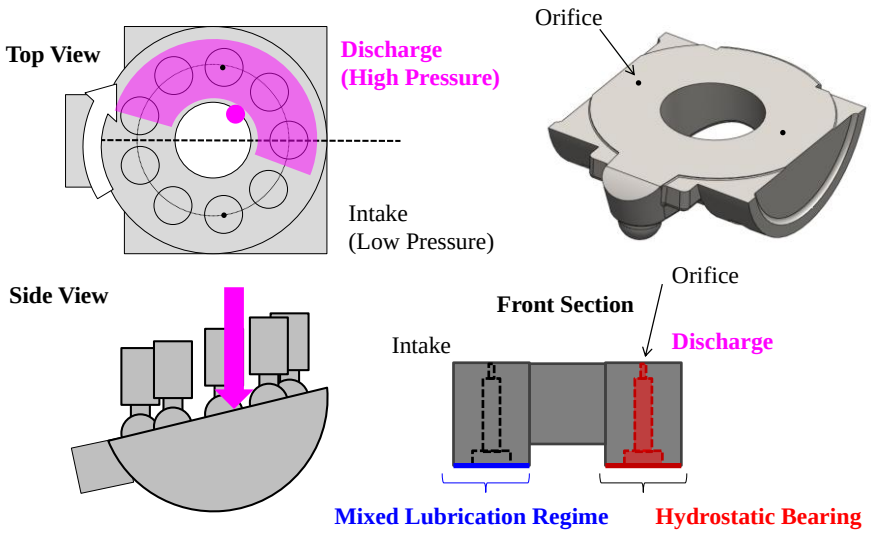

Figure 2. Swash Plate Bearing Layout

The bearing surface on the intake side of the pump does not have sufficient pressure to force fluid across the bearing surface, and therefore, is not a hydrostatic bearing interface. As defined by Miller [2], the bearing under this condition operates in a mixed lubrication regime, and can be characterized as a viscoelastic element with a structural and fluid path, shown in Figure 3, where k are stiffness elements, c are viscous damping elements, $F(t)$ is the transmitted force through the interface, and $x(t)$ is the axial motion of the swash plate.

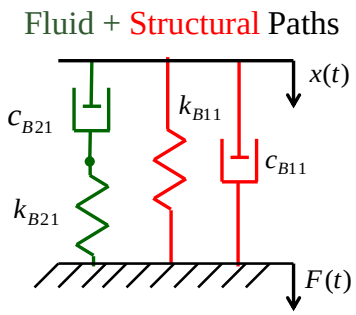

Figure 3. Viscoelastic Contact Model for Intake (Low Pressure) Swash Plate Bearing Interface [2]

The bearing surface on the discharge pressure side of the pump has sufficient fluid pressure to force fluid through the swash plate bearing interface. In this case, the bearing can be considered as a hydrostatic bearing. The hydrostatic bearing interface can be represented by an effective stiffness and damping, which are calculated as a function of pressure and fluid flow over the hydrostatic bearing interface, as illustrated in Figure 4 [4], where p_s is the supply pressure, q_R is the flow rate through the supply orifice into the recess volume, p_R is the recess pressure, q_L is the flow rate through the bearing interface, p_A is the ambient pressure inside the pump housing, and b and L are dimensions of bearing interface.

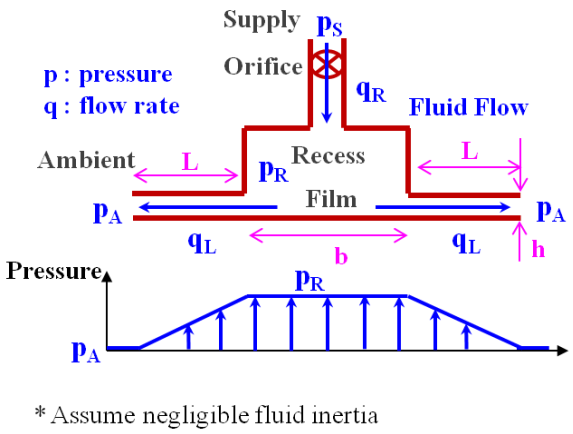

Figure 4. Pressure Distribution over One-Dimensional Hydrostatic Bearing [4]

A failure of the swash plate bearing, such as a clogged orifice due to the build-up of debris within pump due to an ineffective filter, would cause both swash plate bearing interfaces to operate in the mixed lubrication regime. Without an equivalent hydrostatic pressure to react the swash plate and cause it to "float," the high loads produced by the discharge pressure of the pump acting in one direction on the swash plate would increase wear significantly at the bearing interface. This failure could prevent the pump from operating as intended, which requires the bearing to freely rotate to change the swash plate angle.

Chapter 2: Problem Formulation and Methodology

2.1. Problem Formulation

To replicate failure conditions using physical experiments on pumps will be costly and time-consuming. Therefore, in order to better understand the failure mechanisms, specifically of the swash plate bearing, simulation studies are used to

develop a vibration-based health monitoring procedure to predict hydrostatic bearing failure within an axial piston pump. For these experiments, a hydro-mechanical model of the pump will be created using a one-dimensional multi-physics software (MATLAB SimScape [5]). A hydrostatic bearing failure condition will be produced under a variety of simulated operating conditions (such as input shaft speed, swash plate angle, and hydraulic load). This model will not only provide insight into dynamic signatures for this type of failure, but also to changes in force transfer through different structural and hydraulic paths. Creating this procedure requires several steps and experiments. Accordingly, the methods of achieving this health-monitoring procedure for this work will be (i) to develop a one-dimensional multi-physics model of an axial piston pump, (ii) to design and conduct laboratory experiments to obtain model parameters, (iii) to quantify dynamic hydraulic and mechanical loads and paths within the pump under different operating conditions, (iv) estimate acceleration at locations on the pump housing, and (iv) identify acceleration signatures of a simulated swash plate bearing failure, and (v) propose and evaluate a health-monitoring metric based on the virtual pump environment.

2.2. Development of a Multi-Physics Pump Model

First, a one-dimensional multi-physics model of the pump is created to represent the pump and its essential components. This model defines all necessary parameters for calculating hydraulic and dynamic paths in the axial piston pump. It establishes a constant orifice restriction at the output of the pump (which provides a hydraulic load to the pump). The fluid used within the model is defined as Mobil DTE 24 hydraulic fluid,

with properties at 100˚C given Table 1. For these simulations, temperature of the system is assumed to remain constant during its operation. A plate actuator motion constraint is applied to the swash plate to keep the swash plate at a constant angle. At fixed swash plate angles and a constant input shaft speed, this model uses several other subcomponents (as illustrated in Figure 5) to define the pump in detail.

Table 1. Hydraulic Fluid Properties at 100˚C [6]

Property	Value	Units
Fluid density	871	kg/m^3
Kinematic viscosity	5.29	cSt
Bulk modulus at atmospheric pressure and no gas	9.95e8	Pa
Relative amount of trapped air	0.002	--

A single piston subcomponent with valve plate is also created. This piston model includes definitions of the porting plate orifices, which define the angular phasing relations of the intake and discharge porting plate orifices relative to the instantaneous piston location as it travels around the swash plate surface. The swash plate angle dictates the axial position of the piston as it goes through a shaft rotation. These kinematic relationships in turn establish when fluid flow is entering and exiting a given piston.

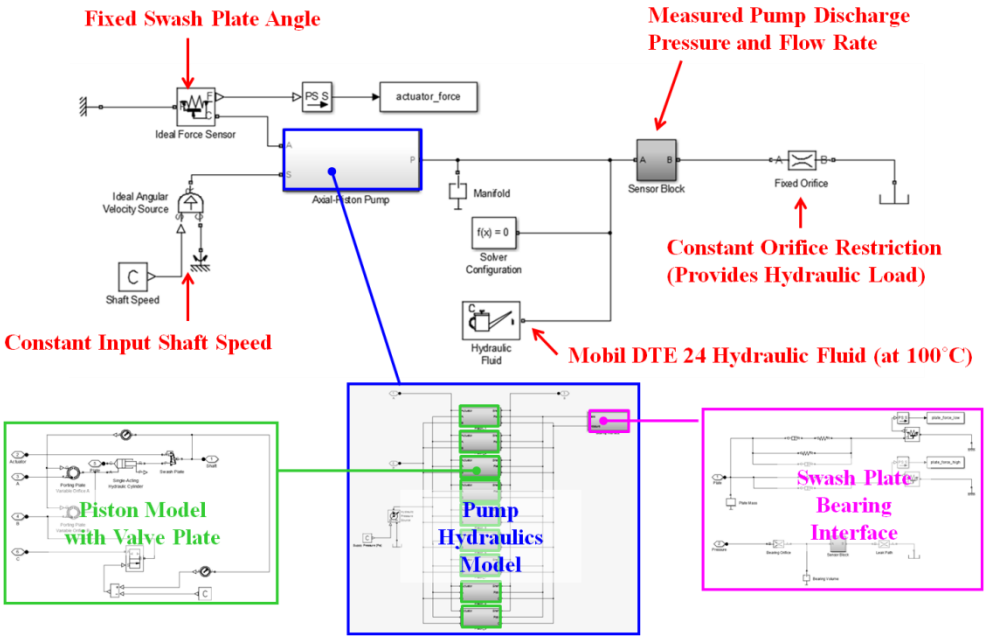

Figure 5. MATLAB SimScape Model of Axial Piston Pump

This piston subcomponent model is integrated within the pump hydraulics model, which for this pump contains nine piston subcomponent models, each phased 40 degrees apart. The rotational motion of the plate is constrained by the control piston actuator and the axial motion of the swash plate is constrained by the swash plate bearing. For a defined constant swash plate angle α, shaft speed Ω, and hydraulic load orifice area A_L, the model calculates hydraulic loads and resulting flow throughout the different subcomponents, as well as the reaction loads at the control piston actuator constraint and swash plate bearing. The low pressure swash plate bearing is modeled using the viscoelastic element shown in Figure 3 and parameters defined by Miller [2]. The hydrostatic bearing is represented by an effective stiffness and viscous damping element in parallel. The flow through the swash plate hydrostatic bearing due to the hydrostatic pressure is calculated by the model and then used to update the effective hydrostatic

bearing stiffness and damping used in the simulation. When there is not sufficient flow through the hydrostatic bearing, the high pressure swash plate bearing reverts to the same element formulation used on the low pressure side. The pump model also calculates the resulting discharge flow rate q_s, discharge pressure p_s, and reaction forces F within the pump. The force transmission paths to the pump housing are assumed to be through the control piston constraint, swash plate bearing interfaces, and force due to the discharge pressure over an effective area A_s of the discharge port. This is illustrated in Figure 6.

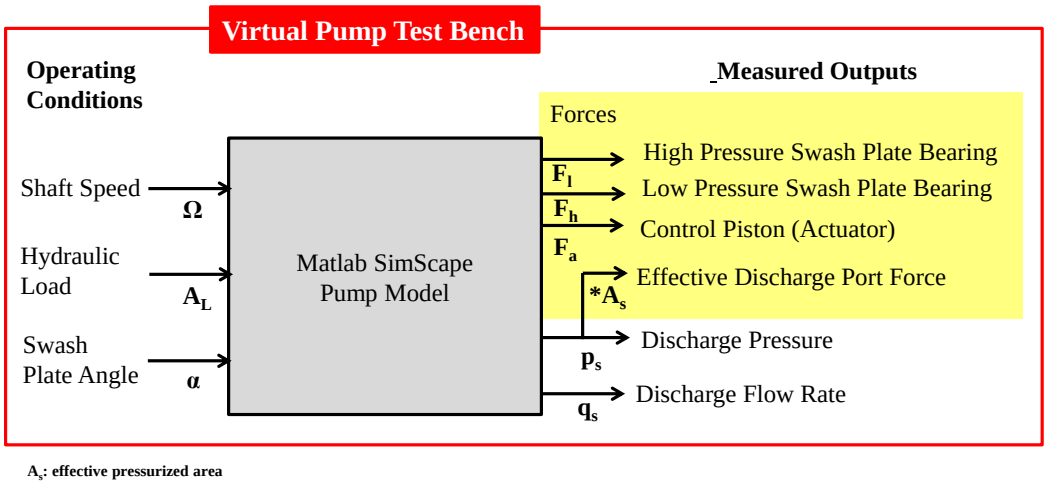

Figure 6. Virtual Pump Test Bench

2.3. Identification of Model Parameters

The model of the axial piston pump requires identification of the kinematic, dynamic, and fluid properties within the pump. The geometry of the pump dictates the parameters necessary for defining kinematic relationships, which are readily calculated using dial calipers. This includes any of the mechanical advantages and phasing relationships in the pump that occur due to the piston arrangement and pump size. The

dynamic parameters of the pump (specifically mass, stiffness, and damping) have already been defined by the interface models characterized by Miller [2].

The fluid properties of the pump, such as flow resistance and compliance, can be found using the pump geometry, assumed fluid parameters, and a set of bench experiments, designed as part of this study. The flow resistances are defined in the pump model as equivalent sharp-edged orifice areas, with negligible inertia and an assumed discharge coefficient of 0.65. There are multiple internal leak paths within the pump. These include the interfaces between the pistons and the barrel, between the barrel and the porting valve plate, between the pistons slippers, which are lumped as an equivalent orifice area A_l. There is also a leakage interface at the swash plate bearing, which is lumped as an equivalent orifice area A_r. These leakage areas affect the discharge pressure and flow rate of the pump as well as the fluid flow through the hydrostatic bearing, and effectively the swash plate bearing interface equivalent stiffness and damping properties. These equivalent orifice areas must be experimentally estimated.

Since a safe means to pressurize the pump using hydraulic fluid was not available, the effective leakage orifice areas for flow restriction are estimated by means of an experimental method using compressed air is used. First, the pump is assembled and pressure ports within the pump are sealed to ensure the only leakage areas are those described above. An air tank is then attached to the discharge port of the pump. Air flow paths into the tank from the compressed shop air and out of the tank to the pump are each controlled by a ball valve. The air tank is pressurized to 686 kPa with the ball valve to the pump close. The shop air ball valve is then closed. The pressure in the tank is measured and recorded using a pressure gage. Finally, the ball valve to the pump is

opened and the time duration to a pressure of 98 kPa is recorded. This setup is conducted for the pump with the swash plate bearing supply orifice plugged and with it unplugged, which is shown in Figure 7.

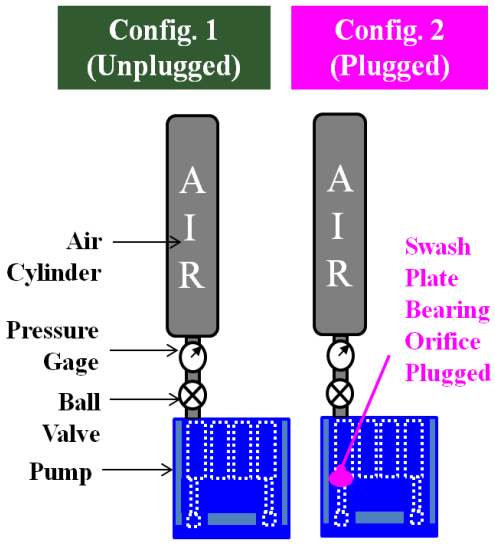

Figure 7: Plugged and Unplugged Configurations of Air Experiment

Two different multi-physics models of this experiment are created in MATLAB SimScape. For the plugged configuration, there is only one leak path (defined as a constant area orifice A_l with the same assumed discharge coefficient as the hydraulic pump model). The physical experiment is duplicated in this simulation environment with only one leak path, and through iteration to match the decay time of the plugged physical experiment, A_l is estimated. For the unplugged configuration, there are two different leak paths (A_l and A_r). A model of the air experiment with these two leak paths is used, with the A_l defined from the plugged configuration. Through iteration to match the decay of the unplugged physical experiment, A_r is estimated.

These tests are conducted at multiple swash plate angles to determine if swash plate angle has significant impact upon effective orifice areas. Angles of 0.26, 0.31, and

0.37 radians (within the operating range of angles) are introduced to the swash plate. Each setup (for plugged and unplugged configuration) is repeated five times for each angle. The calculated average and 95% confidence intervals of the decay times for the air experiments are shown in Figure 8. Using a two-way ANOVA test (significance level = 0.05), it is found that the difference between the plugged and unplugged configurations as well as among different angles is significantly different. A post-hoc Tukey test (significance level = 0.05) is used to determine that the decay times are significantly different for each angle.

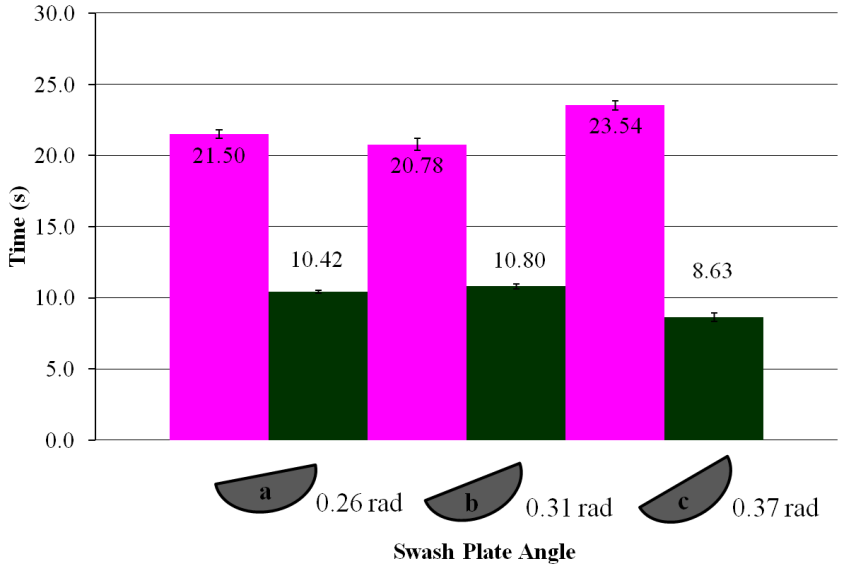

Figure 8. Average Decay Times Using Air Experiments (Magenta: Plugged Configuration, Green: Unplugged Configuration)

Using the average decay times in Figure 8, the effective leakage orifice areas (A_l and A_r) are calculated and shown in Figure 9. As seen in Figure 9, A_l is smaller than A_r for each angle, suggesting a lower flow resistance at the swash plate interface than at other leakage paths. The leakage area A_l is calculated to be between 0.13 and 0.15 mm^2

with discerning trend among angles. The leakage area A_r is calculated to range between 0.16 to 0.24 mm^2, with a maximum value at the highest swash plate angle 0.37 rad. For baseline case of the pump, the effective leakage orifice areas for 0.26 rad are used.

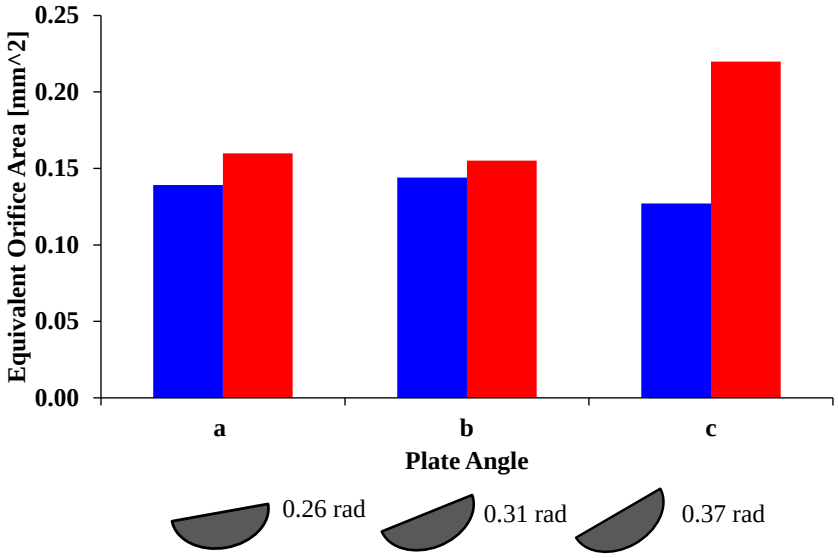

Figure 9. Equivalent Leakage Orifice Areas Estimated Using Experiments (Red: A_r, Blue: A_l)

2.4. Estimation of Acceleration of Pump Housing

For a given set of operating conditions (swash plate angle, hydraulic load orifice area, and shaft speed), the hydraulic pump model calculates discharge pressure and flow rate as well as interfacial forces transmitted to the housing. Interfacial forces are not feasibly measured in a physical pump; however, acceleration of the pump housing is easily measured. The acceleration of the pump housing will contain contributions of all the interfacial force signatures. To extend the defined hydraulic pump model to estimate acceleration on a point on the pump housing, a transfer function relating force to acceleration must be defined, as illustrated in Figure 10.

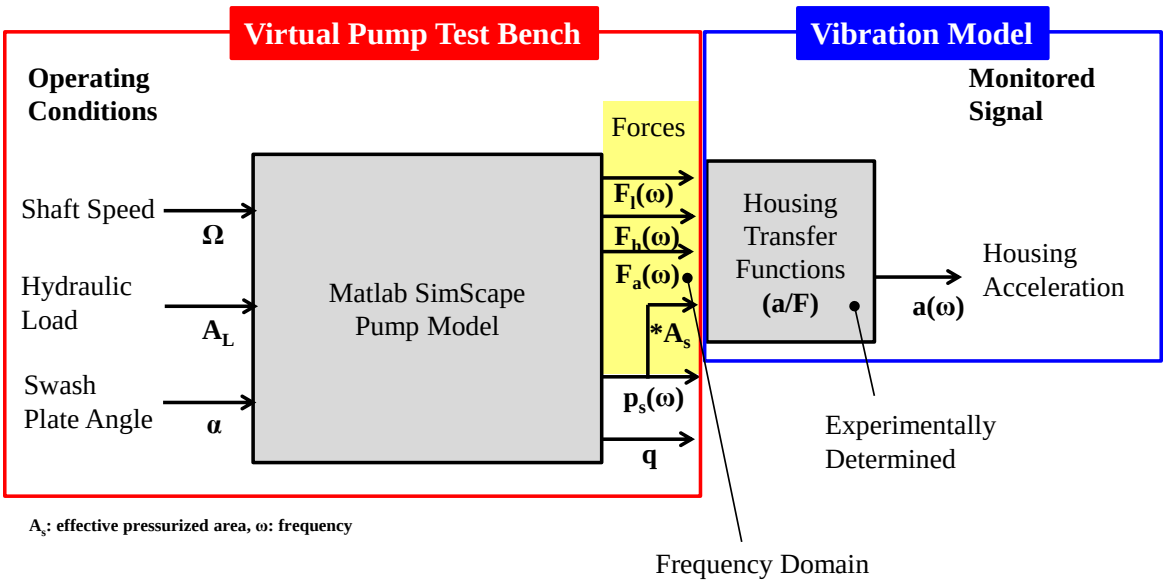

Figure 10. Virtual Pump Test Bench and Vibration Model

If the interfacial forces are transformed to the frequency domain through a Fourier transform (assuming steady state operating condition and constant shaft speed), a set of measured accelerance transfer functions can be used to estimate the acceleration at a point on the housing. This also assumes that housing vibratory motion does not significantly influence the hydraulic system. The resulting acceleration a_o (in frequency domain) at the monitoring location on the pump will be a superposition of the product of each accelerance transfer function and force output from the hydraulic pump model, shown below.

$$a_o = F_l\left(\frac{a_o}{F_l}\right) + F_h\left(\frac{a_o}{F_h}\right) + F_a\left(\frac{a_o}{F_a}\right) + p_s A_s\left(\frac{a_o}{p_s A_s}\right) \qquad (1)$$

Accordingly, accelerance transfer functions are calculated from modal impulse hammer tests. The impulse location is at the assumed accelerometer monitoring location

for the health monitoring procedure. The location is selected to be on the port end of the housing, between the discharge and intake ports due to its observed sensitivity to axial force input at the swash plate bearing. This location is actually found to be more sensitive than locating the accelerometer near the bearing interface on the outer part of the housing. To obtain the accelerance transfer functions, an accelerometer is moved to the different axial force transmission paths (control piston, high pressure bearing, low pressure bearing, and discharge pressure port) and hammer impulse is made at the proposed monitoring location, shown in Figure 11. Due to reciprocity principle in modal measurements, these accelerance transfer functions can be used to relate the interfacial forces from the pump model to the acceleration at the monitoring location on the pump. This method is done since direct impulses could not be made at the interface locations inside the pump. The modal impulse hammer test results are shown in Figure 12.

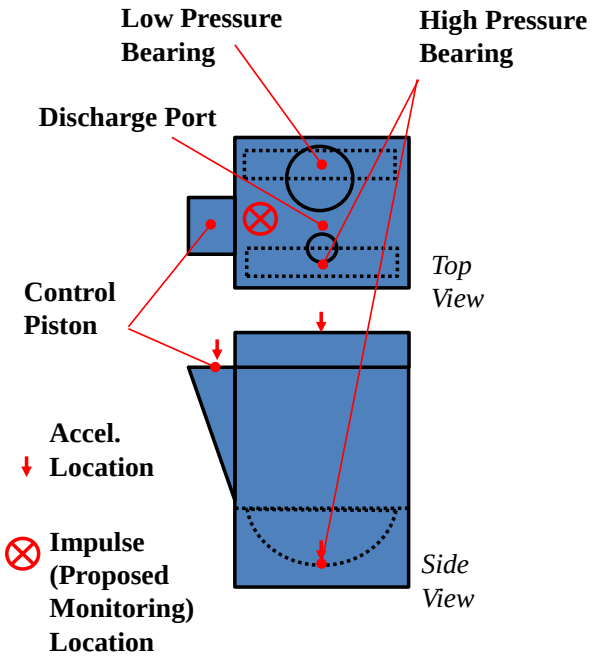

Figure 11. Modal Impulse Hammer Test Setup

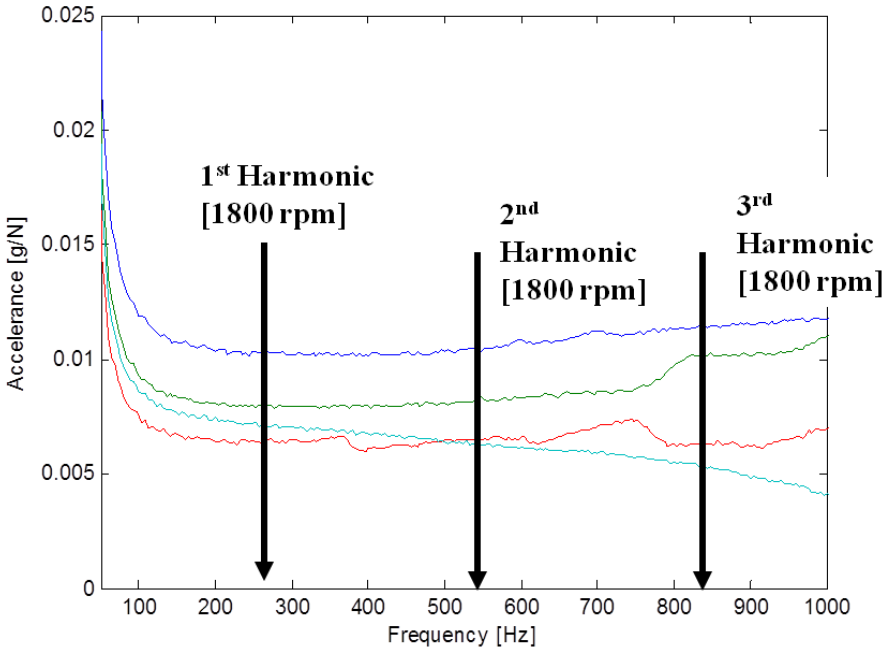

Figure 12. Measured Accelerance at the Four Force Paths (— Control Piston, — High Pressure Bearing, — Low Pressure Bearing, — Discharge Port)

Chapter 3: Results of Virtual Health Monitoring Study

3.1. Simulated Swash Plate Bearing Failure

The healthy (or baseline) model of the pump includes a mixed lubrication regime and a hydrostatic bearing regime under normal operation. Under the modeled failure condition, the supply is cut to 0.001 of the regular nominal area and the bearing interface is modeled as having two mixed lubrication regimes. Essentially, this represents the pump conditions for when the hydrostatic bearing supply orifice is clogged.

The pump simulation is then run under forced failure conditions at a several different operating conditions. The varying operating conditions are driveshaft speeds of

1800 and 2700 rpm and pump loads and load restriction areas of 10, 20, and 30 mm^2. The signatures developed by failure at the hydrostatic bearing are compared against the baseline of the healthy pump to determine metric by which failure could be predicted.

3.2. Force and Pressure Signatures

In time domain, comparing baseline operation to a failure condition reveals several things about the pump. For the discharge pressure signature, variations in operating parameters effect the amplitude and nature of the pump signature; for instance, decreasing A_L noticeably increases the forces upon the pump (Figures 13 and 14). Failure at the hydrostatic bearing supply orifice of the pump, however, is not observable in the discharge pressure signature.

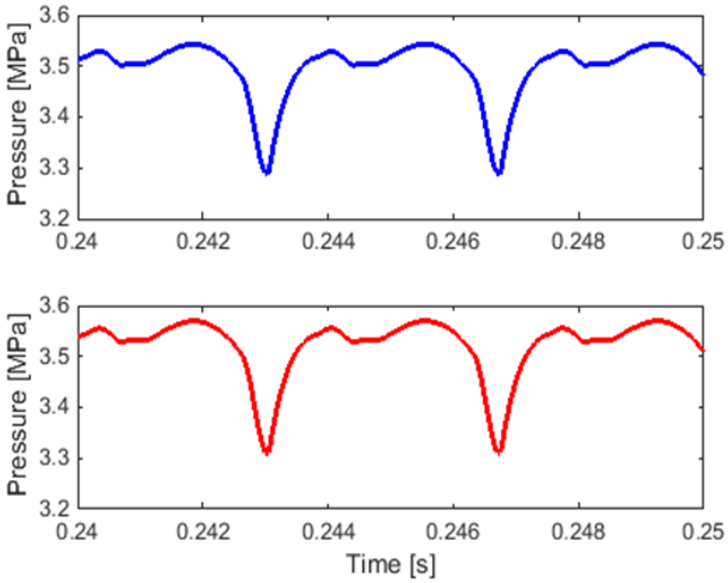

Figure 13. Pressure at High Pressure Bearing Interface for Baseline (Top) and Failure (Bottom) Cases at Ω = 1800 rpm, α = 0.4 rad, A_L = 30 mm^2

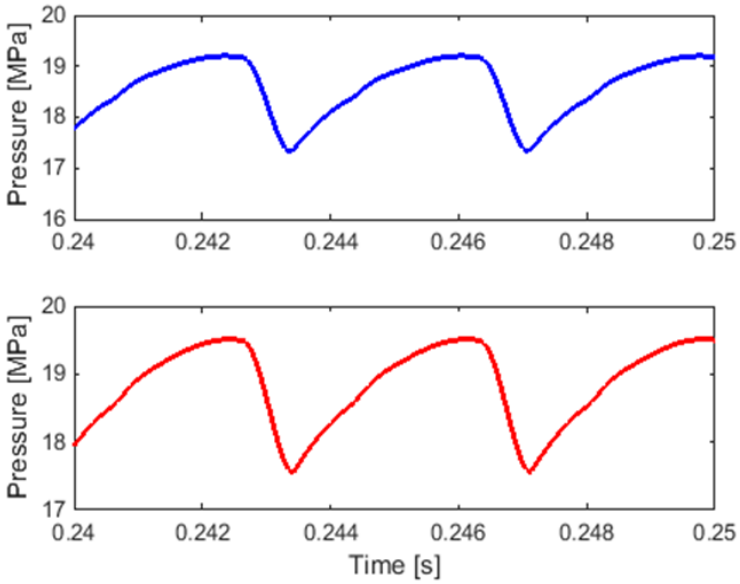

Figure 14. Pressure at High Pressure Bearing Interface for Baseline (Top) and Failure (Bottom) Cases at Ω = 1800 rpm, α = 0.4 rad, A_L = 10 mm^2

In the high pressure bearing force signature, testing at failure conditions reveals that the force signature is dependent upon the operating conditions of the pump, as shown in Figures 15 and 16. Increasing pump load by reducing A_L greatly increases the force transmitted by the pump. In addition, there is a clear change in the pump signature from baseline to failure. Since, however, it is unfeasible to measure forces transmitted to the housing, it is necessary to explore metrics of determining this observed failure signature within the frequency domain.

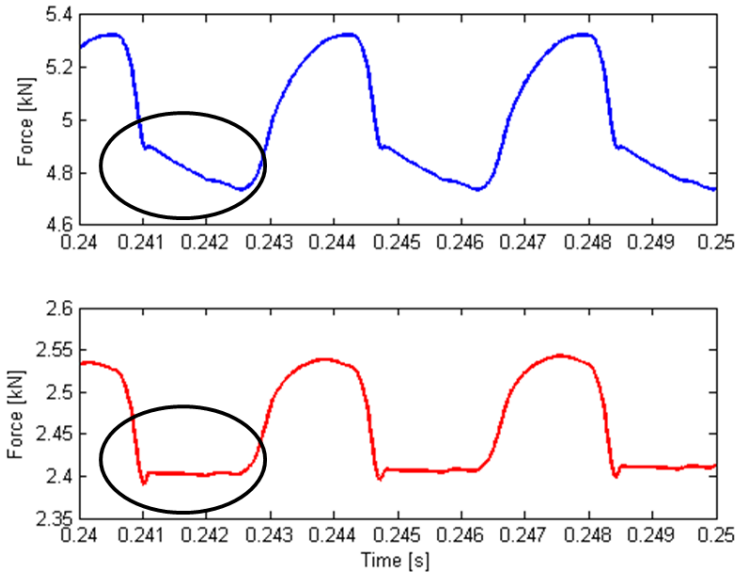

Figure 15. Force at High Pressure Bearing Interface for Baseline (Top) and Failure (Bottom) Cases at Ω = 1800 rpm, α = 0.4 rad, A_L = 30 mm^2

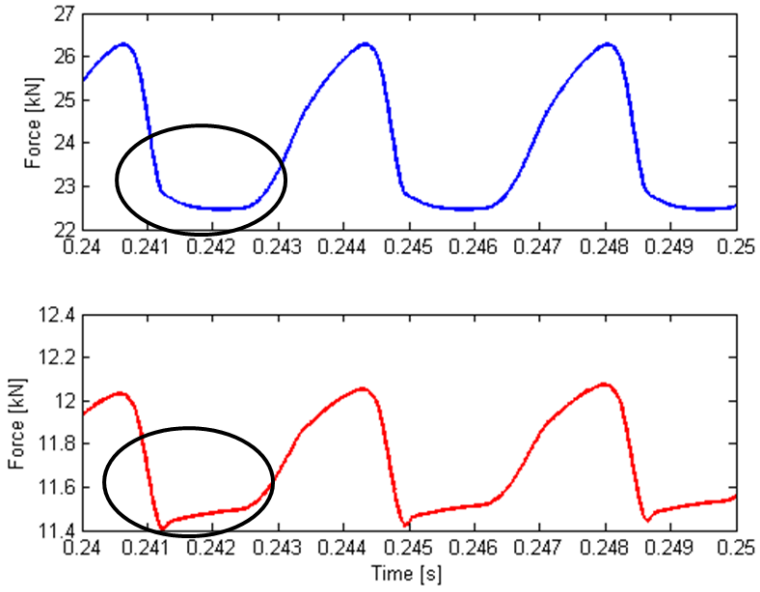

Figure 16. Force at High Pressure Bearing Interface for Baseline (Top) and Failure (Bottom) Cases at Ω = 1800 rpm, α = 0.4 rad, A_L = 10 mm^2

3.3. Definition of Failure Prediction Metrics

For this study, the pump model is run under a given set of operating conditions for three different cases: a baseline case, a failure case due to a clogged hydrostatic bearing supply orifice, and a baseline case with a 20 percent increase in the effective leakage orifice areas (A_l and A_r). This level of variation is observed in the air experiments, and inclusion of this case will help check the robustness of the metric. The spectral contents of the acceleration signal at the different operating conditions are calculated. The spectral contents are reported for the first, second, and third harmonics of the acceleration signature, which occur at the 9-times the shaft speed, due to the presence of 9 pistons. Figure 17 shows that the changes in the first $a(\omega_9)$, second $a(\omega_{18})$, and third harmonics $a(\omega_{27})$ of the acceleration signature at low pressures are generally poor indicators of failure.

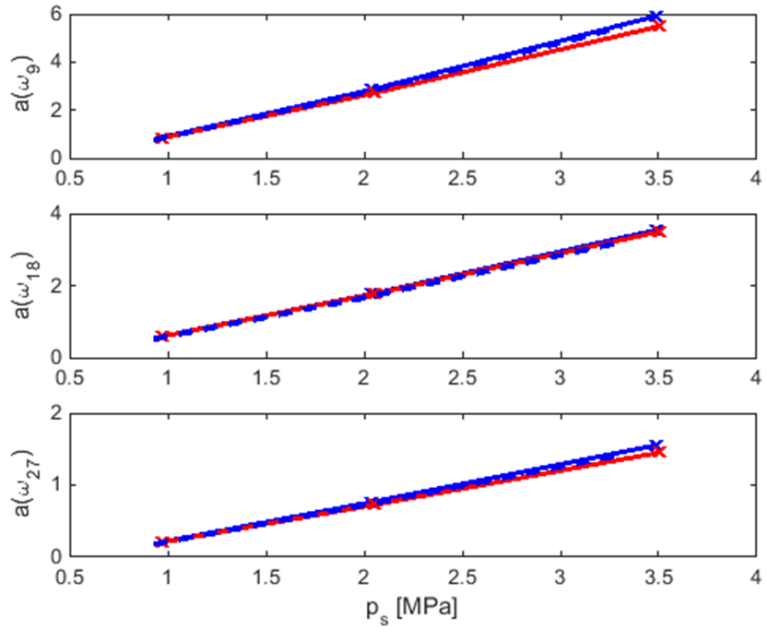

Figure 17. First (ω_9) , Second (ω_{18}), and Third (ω_{27}) Harmonics of Housing Acceleration Spectrum (Units of g's) vs. Discharge Pressures (p_s) (— Baseline, — Failure, --- Baseline with 20% Increase in Effective Leakage Areas) at Ω = 1800 rpm, α = 0.2, 0.3, 0.4 rad, A_L = 30 mm^2

The acceleration signals shown in Figure 17 show a need for a better metric to track failure. Since simply observing frequency changes does not suffice to detect bearing failure, three different metrics is proposed. The first metric I_1, given by

$$I_1 = \frac{a(\omega_{18})}{a(\omega_9)} \qquad (2),$$

observes the change in the second harmonic of the acceleration signal relative to the change in the first harmonic. The second metric I_2, given by

$$I_2 = \frac{a(\omega_{27})}{a(\omega_9)} \qquad (3),$$

observes the ratio of the third harmonic of the acceleration signal relative to the first harmonic.

The third metric I_3, given by

$$I_3 = \frac{a(\omega_{27})}{a(\omega_{18})} \qquad (4),$$

observes the ratio of the third harmonic to that of the second harmonic.

Studies showed that I_1 and I_3 are best at predicting failure at high and low pressures (Figure 18). Generally, the metrics are most sensitive at discharge pressures above 2 MPa. At high and low speeds, I_3 is a clear indicator of failure (Figures 18 and 19). Since it also predicts failure at high and low pressures, I_3 is chosen as the recommended metric to detect bearing failure.

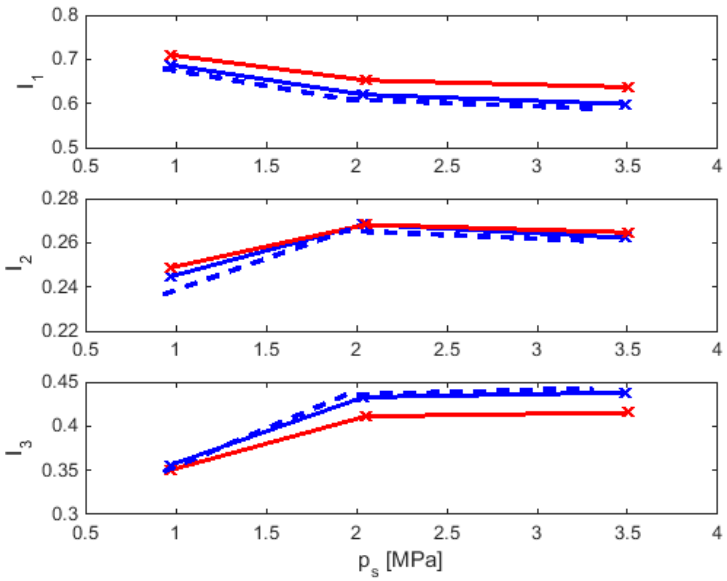

Figure 18. First (ω_9) , Second (ω_{18}), and Third (ω_{27}) Indices vs. Discharge Pressures (p_s) (— Baseline, — Failure, --- Baseline with 20% Increase in Effective Leakage Areas) Cases at Ω = 1800 rpm, α = 0.2, 0.3, 0.4 rad, A_L = 30 mm^2

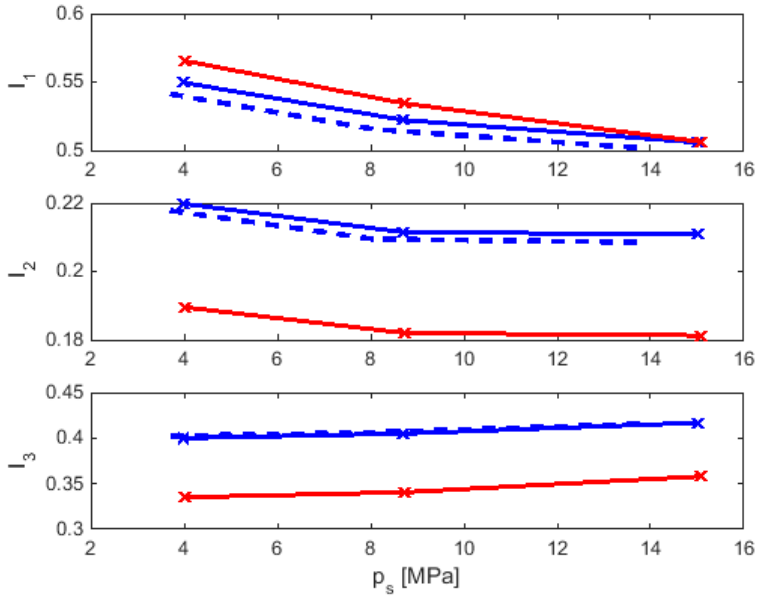

Figure 19. First (ω_9) , Second (ω_{18}), and Third (ω_{27}) Indices vs. Discharge Pressures (p_s) (— Baseline, — Failure, --- Baseline with 20% Increase in Effective Leakage Areas) Cases at Ω = 2700 rpm, α = 0.2, 0.3, 0.4 rad, A_L = 20 mm^2

Chapter 4: Conclusions

A vibration-based health monitoring metric is proposed to identify hydrostatic bearing failure using a virtual pump model. The metric consists of the ratio of the third to second harmonic of the acceleration signature. To implement this procedure, an algorithm will require tracking of the metric along with the mean discharge pressure and input shaft speed. It consistently detects hydrostatic bearing failure under a wide range of pump operating conditions and is insensitive to experimentally quantified variation in the pump model parameters. The system offers a procedure for predicting failure that does not first rely upon initial physical testing. This procedure augments the costs of

empirically testing for failure on physical tests and provides more insight than determining failure post hoc.

4.1. Model Limitations

Several assumptions are used in the development of this procedure. For the pump simulations, temperatures of the system are assumed to remain constant during its operation. The flow resistances are defined in the pump model as equivalent sharp-edged orifice areas, with negligible inertia and an assumed discharge coefficient of 0.65. The process assumes steady state operating conditions and constant input shaft speed within the pump. Furthermore, it assumes that the housing vibratory motion does not significantly influence the hydraulic system, and the four force transmission paths into the housing are assumed to be uniaxial.

Although promising results are demonstrated using this virtual pump model, this procedure has not yet been evaluated in the presence of extraneous inputs due to other component dynamics within the applied system. Therefore, the virtual pump model, associated assumptions, and health monitoring procedure should be experimentally validated in the future.

4.2. Future Work and Applications

This model could be expanded in several ways. The four assumed one-dimensional force transmission paths could be refined with increased fidelity by defining load distribution paths or including multi-dimensional interface properties. Additional inertia effects of the bodies and the fluids could be included by refining the hydraulic model to include fluid inertance and implementing the mechanical elements within a

multi-body dynamics formulation. The model could be modified to monitor additional types of failure, such as that of the roller bearings on the driveshaft, by including representations of the load paths through those elements.

This model provides an environment suitable to isolate specific kinds of failures and gain a deeper understanding into these failures. In addition, this model provides important information regarding the hydraulic and mechanical transmitted load paths within the pump that could not be directly measured without radically altering the physical pump. Due to the parametric nature of the model, the defined health monitoring procedure could be applied to pumps of various sizes and geometries as well as to different hydraulic fluids. The virtual pump monitoring procedure could be used to detect improper usage, such as using a different hydraulic fluid other than one specified, or to quantify wear within the pump (associated with the equivalent leakage orifice areas in the model). Vibration signatures could also be correlated to the acoustic noise at certain operating conditions, which might be useful in cases where a vibration transducer is not available. The robustness of the procedure could also be further investigated by altering the effective leakage orifice areas at different operating conditions (swash plate angle, mean discharge pressure, piston position, shaft rotational angle, etc.).

Ultimately, this work serves as an example of defining and evaluating health monitoring metrics in a virtual environment. Aspects and extensions of this research could ultimately be used by pump manufacturers to provide preventative maintenance guidelines, to identify the least damaging and quietest pump operating regimes, and to screen design concepts before building prototypes.

References

[1] Eaton Corp, *620 Mobile Piston Pump Catalog*, 2013 [Online], Available: http://www.eaton.com/ecm/groups/public/@pub/@eaton/@hyd/documents/content/pll_1427.pdf

[2] A. C. Miller. "Assessment of Alternate Viscoelastic Contact Models for a Bearing Interface between an Axial Piston Pump Swash Plate and Housing", M.S. thesis, Dept. Mech. And Aero. Eng., Ohio State Univ., Columbus, OH, 2014.

[3] A. G. Piersol and T. L. Paez, *Harris's Shock and Vibration Handbook*, Sixth Edition, New York: McGraw Hill, 2010.

[4] S. Andrés. Course Notes on Hydrostatic Bearings. Texas A&M, 2010.

[5] *MATLAB SimScape*. Computer software. Mathworks, Inc., 2014. Retrieved from <http://www.mathworks.com/products/simscape/>

[6] Exxon Mobil Corp., *Mobil DTE™ 20 Series Hydraulic Oils*, 2014 [Online], Available: http://www.mobil.com/USA-English/Lubes/PDS/GLXXENINDMOMobil_DTE_20_Series.aspx

List of Symbols

A_L --Hydraulic load orifice area [m^2]

A_l -- Effective leak area for plugged configuration [m^2]

A_r -- Effective leak area for unplugged configuration [m^2]

A_s -- Effective pressurized area [m^2]

a -- Pump housing acceleration [m/s^2]

B -- Length of bearing [mm]

b -- Bearing recess width [mm]

c -- Viscous Damping [Ns/m]

F -- Force [N]

F_a -- Force on actuator [N]

F_h -- High pressure bearing force [N]

F_l -- Low pressure bearing force [N]

k -- Stiffness [N/m]

L -- Bearing width [mm]

p_A -- Ambient intake pressure [MPa]

p_R -- Recess pressure [MPa]

p_s -- Discharge pressure [MPa]

q_L -- Flow through bearing interface [L/min]

q_R -- Bearing recess flow rate [L/min]

q_s -- Discharge flow rate [L/min]

t -- Time [s]

x -- Axial motion of swash plate [m]

α -- Plate angle [rad]

Ω -- Input shaft speed [rev/min]

ω -- Angular frequency [rad/s]